ELSEVIER

Journal of Nuclear Materials 274 (1999) 84–90

journal of nuclear materials

www.elsevier.nl/locate/jnucmat

Transmutation of actinides in inert-matrix fuels: fabrication studies and modelling of fuel behaviour

R.J.M. Konings *, K. Bakker, J.G. Boshoven, H. Hein, M.E. Huntelaar, R.R. van der Laan

NRG, P.O. Box 25, 1755 ZG Petten, The Netherlands

Abstract

A review of the ongoing research of inert-matrix fuels for the transmutation of actinides is given. Three fabrication routes are described, co-precipitation (CPP), low-impact mixing of powders (LMP) and mixing of particles and powders (MPP). These methods have been tested for various combinations of actinide host materials and inert matrices. Most attention is given to a fuel concept consisting of an actinide-containing host phase and spinel as the inert matrix. To understand the phase relations and melting behaviour of this hybrid fuel type the binary phase diagrams in the system $(Zr,Y,Pu)O_2$ + $MgAl_2O_4$ are being modelled and some results are presented. In addition, the thermal behaviour of $MgAl_2O_4$-based inert-matrix fuels is investigated. The thermal conductivity of polycrystalline spinel is measured and in-pile temperature measurements of an UO_2 + $MgAl_2O_4$ target are analysed. © 1999 Elsevier Science B.V. All rights reserved.

1. Introduction

Within the frame of the research programme of NRG for innovative options for the back-end of the fuel cycle, inert-matrix fuels for transmutation of actinides such as plutonium and americium are being studied extensively. The work covers the study of the fabrication of targets for in- and out-of-pile tests in the recently constructed actinide laboratory, modelling of fuel behaviour, irradiation tests in the HFR and post-irradiation examinations in the hot-cell laboratory in Petten.

The research at NRG is focused on dispersion-type fuels in which the actinide phase is distributed as a separate phase in a so-called inert matrix. This concept has evolved as one of the most promising, as is explained in detail in Ref. [1]. Though ceramic oxides, carbides and nitrides as well as metals are considered as the inert matrix, our activities in the field of fabrication studies, modelling and irradiation experiments have been restricted to oxide matrices so far. At present we consider ZrO_2, Y_2O_3, MgO, $MgAl_2O_4$ and $Y_3Al_5O_{12}$ to be the most promising materials, based on criteria concerning their neutronic properties, the fabrication and processing of the materials, the physico-chemical properties and their compatibility with existing reactor technology, as discussed in detail by Cocuaud et al. [2].

In the present paper we will present the progress of our research activities in the field of uranium-free fuels, with emphasis on the results of the fabrication of targets and modelling of fuel behaviour. The results of our extensive irradiation programme on inert-matrix fuels will only be discussed shortly since the irradiation experiments and post-irradiation examinations are on-going. Results of studies of neutron irradiation of pure inert matrix materials are reported in a second paper at this Workshop [3].

2. Fuel fabrication

Three different routes for the fabrication of dispersion-type uranium-free fuels are being investigated at our laboratory (Fig. 1), using uranium, cerium and thorium as substitutes for plutonium and americium.

---

* Corresponding author. Present address: CEC Joint Research Centre, Institute for Transuranium Elements, P.O. Box 2340, 76125 Karlsruhe, Germany.

0022-3115/99/$ – see front matter © 1999 Elsevier Science B.V. All rights reserved.
PII: S0022-3115(99)00043-4

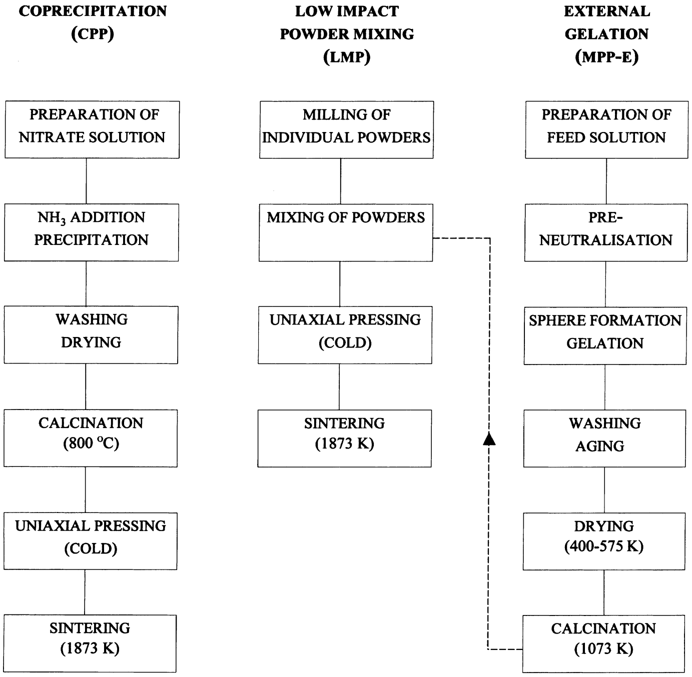

Fig. 1. Schematic flow diagrams of the fabrication processes for hetrogeneous fuels.

- co-precipitation (CPP);
- low-impact mixing of powders (LMP);
- mixing of particles and powder (MPP).

The CPP route is a relatively simple one, based on the dissolution of the starting materials in nitric acid and the precipitation of all the components from this solution after adjusting the pH by the addition of ammonia. The powder, obtained after washing, drying and calcination of the precipitate, is directly used for the preparation of pellets. Ceramographic analysis, SEM and X-ray radiography showed that the actinide phase is present as very small (sub-micron size) particles in the matrix, uniformly distributed in the pellets (Fig. 2).

The LMP route is based on the low-impact mixing of a sinter-active powder of the inert matrix and the powder of the actinide phase. The low-impact mixing is performed manually in a mortar (initial trials) or mechanically in a mixer mill (Retsch, MM-2000). The blend thus obtained is used for the preparation of pellets. This method has been tested for matrix materials mixed with a single oxide phase or mixed with a solid solution of two or more oxides. Ceramographic analysis showed that for all mixtures of inert matrix and UO_2 investigated, a dispersion of the actinide phase has been obtained, randomly distributed in the matrix. However, the major part of the UO_2 is found in irregularly shaped inclusions whose size is in the order of 100–200 μm, a small fraction is present as small inclusions of >10 μm (Fig. 3).

The MPP route is the most complex one that has been investigated. It is based on the fabrication of particles containing the actinide phase by sol–gel technique followed by mixing of the particles and matrix powder. In our laboratory, the external gelation method is the

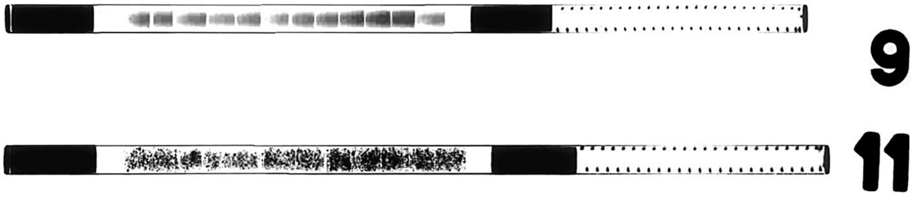

Fig. 2. X-ray photographs of $MgAl_2O_4$ + UO_2 targets for the T3 irradiation experiment in the HFR showing the distinct difference in size and distribution of the UO_2 inclusions; top, pellets prepared by CPP; bottom pellets prepared by MPP. The length of the capsules is 168 mm.

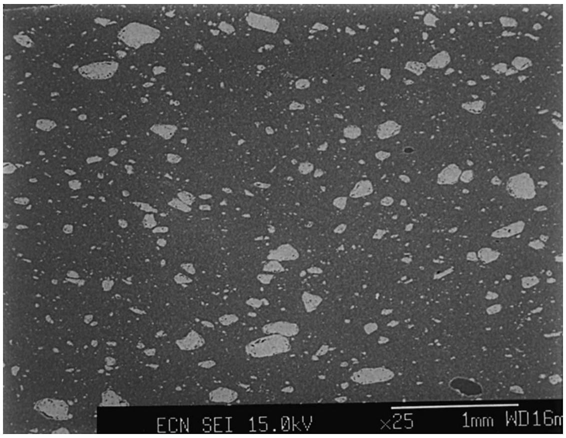

Fig. 3. Dispersion of UO_2 in a matrix of spinel prepared by LMP.

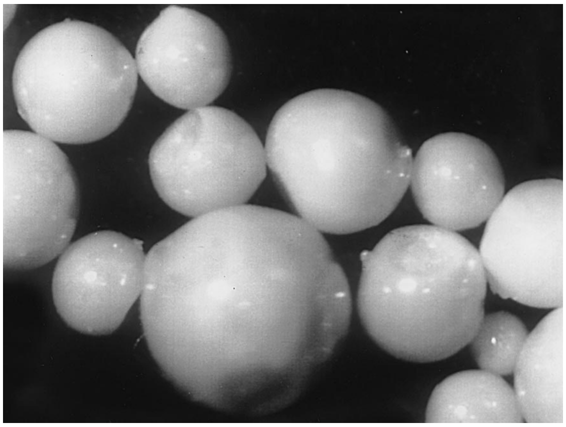

Fig. 4. ThO_2 "spheres" prepared by external gelation method.

reference method for the sol–gel process (MPP-E). It is based on the injection of droplets of a nitrate solution in an organic phase (keton), sphere formation in the organic phase and gelation in the ammonia phase [4]. After washing and drying the spheres are calcined and, optionally, sintered. Spherical particles with a controlled and uniform size (200–300 μm) can be prepared by this method (Fig. 4). Next, the particles are mixed with a sinter-active powder as described above for the LMP route, using zinc stearate and camphor as additives. This approach has been investigated for ThO_2 spheres prepared at NRG and $(Zr,Y,Ce)O_2$ spheres prepared by the internal gelation method at the Paul Scherrer Institute [5], using $MgAl_2O_4$ as the matrix. Both calcined and sintered spheres have been used for this purpose. Ceramographic analysis and SEM showed that calcined spheres gave the best results. The use of sintered spheres resulted in a ring of microcracks (up to 40 μm in length) perpendicular to the sphere-matrix interface (Fig. 5), although this effect can be minimised by decreasing the heating rate during the sintering. The general observations are as follows.

1. As a result of the much larger volume decrease of the matrix compared to the sphere during sintering, an irregular surface of the pellet was obtained, caused by protruding of the spheres out of the surface (up to 60 μm, as obtained by profilometry of the surfaces).
2. The spheres are not uniformly distributed in the matrix but concentrate during the loading of the mixture in the press, probably due to the difference in density between particles and powder.
3. Spheres touch and agglomerate.

The protruding of spheres can easily be solved by a mechanical treatment of the surface of the sintered

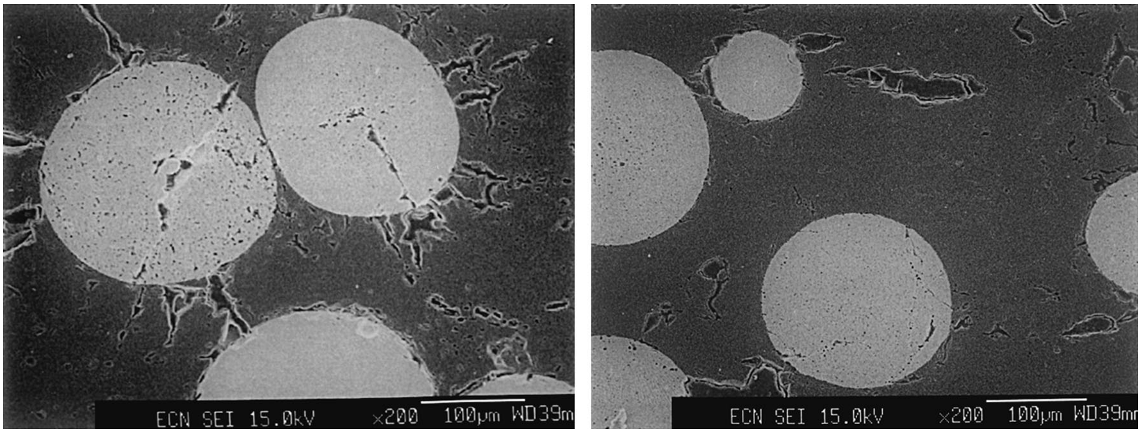

Fig. 5. Dispersions of spheres of $(Zr,Y,Ce)O_2$ in a matrix of spinel (sintered at 1875 K in argon); left, sintered spheres used as starting material; right, calcined spheres used as starting material. The spheres were prepared by an internal gelation process at PSI (Switzerland).

pellets although this will lead to scrap that needs to be recycled and, moreover, the formation of dust containing the actinides. This might be acceptable for plutonium fuels, but it is not to be preferred for americium fuels. The concentration and agglomeration of spheres will probably lead to hot spots in the fuel that need to be avoided. Studies have therefore been started to minimise the above noted effects.

3. Thermodynamic modelling of the $(Zr,Y,Pu)O_2$ + $MgAl_2O_4$ system

An activity has been started to model the chemical equilibria in the $(Zr,Y,Pu)O_2$ + $MgAl_2O_4$ system in order to understand the phase relations and melting behaviour of such a fuel. To that purpose the systems Al_2O_3–PuO_2, MgO–PuO_2 and ZrO_2–PuO_2 have been modelled with MTDATA [6] and the Lukas programmes [7], whereas the system Y_2O_3–PuO_2 has been reviewed (Table 1).

The system Al_2O_3–PuO_2 has been reported to be a simple eutectic one by Hough and Marples [8] and is modelled using a sub-regular solution model [12]. For the system MgO–PuO_2, which is also a simple eutectic one, limited solid solubility of MgO in PuO_2 was reported [8]. To model this, an association model was applied and the association parameters were transposed from the MgO–CeO_2 system [12].

The system ZrO_2–PuO_2 has been investigated by Carroll in 1963 [9]. The results of this study are, however suspect because of incomplete and erroneous observations. The melting point of PuO_2 is reported to be 2570 K, about 100 K lower than the currently accepted value. Considering the conditions applied in the experiments by Carroll, it is likely that the PuO_2 was reduced to $PuO_{1.61}$. On the ZrO_2 part of the system the phase relations are not in agreement with those in pure ZrO_2. The reported monoclinic to cubic transition should be the monoclinic to tetragonal one. We have therefore not used the results of Carroll for the modelling of this system and have used the much better known ZrO_2–CeO_2 system to simulate the description of ZrO_2–PuO_2 system [13]. This resulted in the phase diagram shown in Fig. 6.

Table 1
Summary of the systems included in the thermodynamic modelling

System	Experimental data		Remarks
	Solid state	Liquid	
Al_2O_3–PuO_2	–	Ref. [8]	Simple eutectic
MgO–PuO_2	–	Ref. [8]	Modelled after MgO–CeO_2
ZrO_2–PuO_2	Ref. [9]	Ref. [9]	Modelled after ZrO_2–CeO_2
$YO_{1.5}$–PuO_2	Ref. [10]	–	No acceptable model available
$YO_{1.5}$–ZrO_2	See Ref. [11]	See Ref. [11]	Model by Jin and Du [11] accepted

From the binary phase diagram, ternary ones can be constructed. Fig. 7 gives an example of the isopleth section for the face-centered-cubic phase (PuO_2 with some limited solubility of MgO) and the spinel phase ($MgAl_2O_4$) as derived from the ternary PuO_2–MgO–Al_2O_3 system [14]. It can be seen that in the composition range 0–14 mol% PuO_2, the liquidus temperature of the

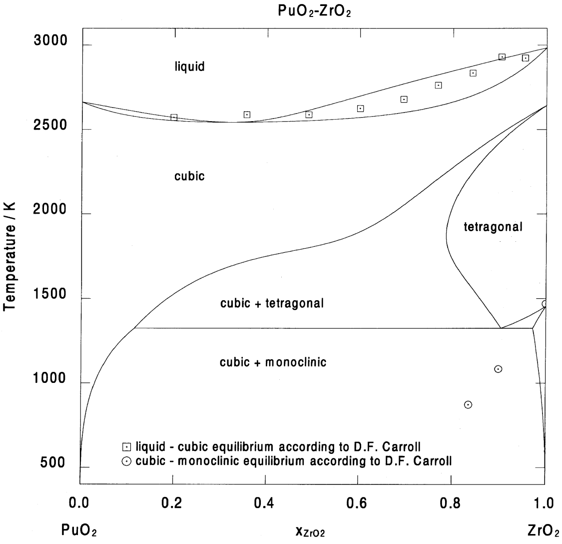

Fig. 6. The calculated phase diagram of the system PuO_2–ZrO_2.

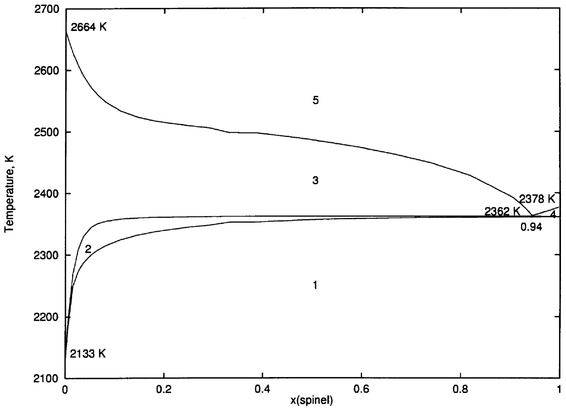

Fig. 7. The isopleth section PuO_2–$MgAl_2O_4$ as derived from the ternary system PuO_2–MgO–Al_2O_3; 1 = fcc + spinel; 2 = fcc + spines + Liquid; 3 = Liquid + fcc; 4 = Liquid + spinel; 5 = Liquid. fcc represents the cubic solid solution phase $(Pu^{4+}, Mg^{2+}, Va)O_2$ where Va means vacancy.

fuel is close to the eutectic temperature of the system, 2362 K and the melting point of $MgAl_2O_4$, 2378 K. At the PuO_2 rich side of the system, however, a steep change in the liquidus temperature occurs.

4. Analysis and modelling of the thermal conductivity of spinel

In September 1997 the T4ter irradiation experiment was started in the High Flux Reactor (HFR) at Petten. In this experiment a stainless steel capsule containing a heterogeneous dispersion of UO_2 (10.5% in volume, 20% enriched in ^{235}U) in $MgAl_2O_4$ prepared by the CPP technique, is being irradiated in a central core position of the HFR. During the irradiation the central temperature of the fuel, measured by a type K thermocouple inserted in a niobium tube, and the temperature of the aluminium sample holder are recorded. Using these values a first attempt is made to model the behaviour of the fuel.

But first it was necessary to determine the thermal conductivity of the $MgAl_2O_4$ used for the fabrication of targets since literature data show a considerable variation for $MgAl_2O_4$ samples of different sources. Using the laser-flash method, the temperature dependence of the thermal conductivity of a sintered polycrystalline $MgAl_2O_4$ sample was measured in the range 298–1050 K. The results of these measurements are shown in Fig. 8.

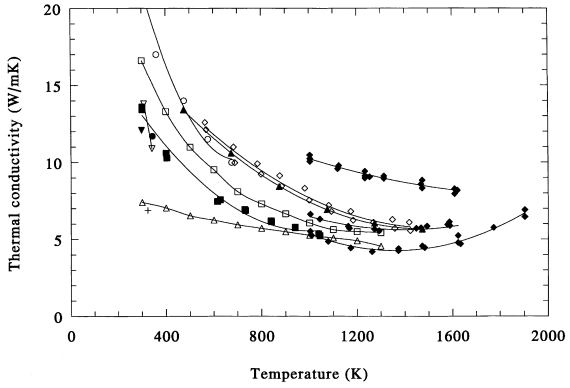

Fig. 8. The thermal conductivity of $MgAl_2O_4$, recalculated to 100% density: ■, present study; □, Schulz and Haase, sample 1 [15]; △, Schulz and Haase, sample 2 [15]; ○, Burghartz and Schulz [16]; ▽, McCarthy and Ballard [17]; ▲, Kingery et al. [18]; ●, Weeks and Seifert [19]; ◇, Norton and Kingery [20]; ♦, Rudkin [21]; ▼, Taylor [22]; +, Jaeger et al. [23].

Table 2
The measured and calculated temperature difference (ΔT) between the cladding and central fuel temperature in the T4ter experiment

Cycle	Cumulative full power days	T_{central} (K) average	$\Delta T_{\text{measured}}$ (K)	$\Delta T_{\text{calculated}}$ (K)
1	25.58	1273	416	409
2	50.88	1273	403	356
3	76.22	1273	366	329
4	101.67	1208	356	240
5	127.01	1173	349	208
6	152.37	1103	329	219
7	175.82	1225	378	212
8	200.86	1133	320	200
9	226.05	1053	283	180
10	251.34	1087	315	175
11	275.09	1036	299	148

For the first 11 irradiation cycles of the T4ter experiment the temperature difference ΔT between the thermocouple position in the fuel and in the sample holder is compared to the calculated value obtained from a finite-element model of the sample and the sample holder. The preliminary results are shown in Table 2 together with the measured values. It can be seen that for cycle 1 a good agreement is obtained between the measured and calculated ΔT but that the agreement becomes progressively worse for the subsequent cycles. This can be explained by the following factors.

- The thermal conductivity of the mixture, and especially the $MgAl_2O_4$ matrix decreases as a result of radiation damage in the lattice caused by neutrons and fission fragments.
- The release of the fission gases Xe and Kr, which have a much lower thermal conductivity than the filling gas helium (1 bar at room temperature), as a result of which the overall thermal conductivity of the gas in the gap between the pellets and the cladding decreases.

The dispersion size of the UO_2 is important for both cases. Due to the small size of the UO_2 particles (<1 μm) most of the fission fragments penetrate the $MgAl_2O_4$ matrix since the reach of the fission products is about 8–10 μm. As a result the total matrix is subjected to the damage induced by the fission fragments, which is significantly more prominent than the damage introduced by neutrons. Because most of the fission fragments penetrate the matrix, the fission gas retention in this fuel depends mainly on the gas retention properties of $MgAl_2O_4$ (which are poorly known) and less on the gas retention properties of UO_2 (which are very good).

The magnitude of the fission-gas release from the fuel as well as of the decrease of the thermal conductivity of the fuel due to irradiation are yet unknown and, hence, it is not possible to indicate which effect has the main influence on ΔT. Sensitivity calculations show that a decrease of the thermal conductivity of $MgAl_2O_4$ by a factor of four after 11 cycles might explain the

Table 3
Evaluation of the three fabrication routes studied for the fabrication of targets for transmutation of actinides

Technique	Advantages	Disadvantages
Co-precipitation (CPP)	Easy Little radioactive dust	Small particle size Not possible to add stabilising host
Low-impact mixing of powders (LMP)	Easy	Non-uniform dispersion size Radioactive dust formation
Mixing of particles and powders (MPP)	Control of dispersion size Little radioactive dust	Complex operation Agglomeration of particles Surface effects

difference. However, the difference might also be explained by a fission-gas release of about 6% after 11 cycles. Final conclusions must wait for the results of post-irradiation examinations of the target.

5. Discussion

As presented in previous papers [1,24], the 'ideal' dispersion-type fuel has the following characteristics.

- Spherical inclusions of a size between 50 and 300 μm to minimise the volume of the matrix that is subjected to the bombardment of fission fragments and, as a result, limit the radiation damage (which decreases the thermal conductivity of spinel).
- A random distribution of isolated spheres to avoid hot spots in the fuel.
- A stabilising 'host' phase for the actinide spheres to retain the activation and fission products, especially at a high burnup.
- An inert matrix of a good thermal conductor to maximise the allowable fission rate and limit the central fuel temperature.

The results of the fabrication studies presented here (Table 3) show that the CPP method cannot meet these requirements. The submicron size of the inclusions will lead to a high degree of damage of the inert matrix which in turn will affect the thermal conductivity and/or the fission-gas release of the matrix, as shown in the analysis of the T4ter experiment. Moreover, it is difficult to add a stabilising 'host' to the actinide phase by this method. The LMP method can meet these requirements much better. However, our experience gained so far shows that the control of the inclusion size and shape is limited and that the presence of some small ones cannot be avoided. The MPP method offers the best possibilities to control sphere size, though it is a more complex dual route (sol–gel and powder mixing). Unfortunately, we are presently not able to achieve sufficient control of the particle distribution and the surface effects with the MPP method.

With respect to the choice of materials, the number of candidates is limited, considering the pre-selection presented by the EFTTRA group [2] who identified ZrO_2, Y_2O_3, MgO, $MgAl_2O_4$ and $Y_3Al_5O_{12}$ as the most promising ones. Of these only MgO, $MgAl_2O_4$ and $Y_3Al_5O_{12}$ form a two phase mixture with the actinide oxides, and can be considered as matrix materials; MgO being suited for fast reactors only as it is not compatible with water. ZrO_2 and Y_2O_3 form solid solutions with the actinide oxides and yttria-stabilised zirconia seems therefore to be the most suitable 'host' for the actinides.

The fuel concept for plutonium burning in PWRs that evolves from this discussion consists of $(Zr,Y,Pu)O_2$ spheres in a matrix of $MgAl_2O_4$ or $Y_3Al_5O_{12}$, the so-called 'hybrid' fuel concept [1]. Knowledge of the chemical behaviour of this fuel, especially as a function of burnup, is important to assess this concept. Apart from irradiation experiments, this information can be obtained from thermodynamic models, as presented here for the $MgAl_2O_4$ + $(Zr,Y,Pu)O_2$ system. Though the thermodynamic model to describe the behaviour of this system in the solid and liquid state is not yet complete, mainly due to insufficient data, the results obtained so far show that the 'hybrid' concept for PWR fuel ($<10^{v}$% PuO_2) does not lead to unacceptable changes in the phase relations and melting behaviour. However, this thermodynamic model represent the fuel at beginning-of-life. The formation of fission products and the related change in oxygen potential can influence the chemical equilibria significantly, especially at the host–matrix interface. In our future work this aspect will be taken into account.

Acknowledgements

This work was sponsored by the Dutch Ministry of Economic Affairs (FAS-number 62373).

References

[1] N. Chauvin, R.J.M. Konings, Hj. Matzke, these Proceedings, p. 105.

[2] N. Cocuaud, E. Picard, R.J.M. Konings, A. Conti, Hj. Matzke, in: Proceedings Global'97, Yokohama, October 1997, p. 1044.
[3] E.A.C. Neeft, R.J.M. Konings, K. Bakker, J.G. Boshoven, H. Hein, R.P.C. Schram, A. van Veen, R. Conrad, these Proceedings, p. 78.
[4] H. Ringel, Kernforschungsanlage Jülich, Report Jül 1258, December 1975.
[5] M. Burghartz, G. Ledergerber, F. Ingold, T. Xie, F. Botta, K. Idemitsu, presented at 4th Inert Matrix Fuel Workshop, Villigen, Oct. 1998.
[6] R.H. Davies, A.T. Dinsdale, J.A. Gisby, S.M. Hodson, T. Barry, MTDATA Handbook: NPL Databank for Metallurgical Thermochemistry, 1994.
[7] H.L. Lukas, S.G. Fries, J. Phase Equil. 13 (1992) 532.
[8] A. Hough, J.A.C. Marple, J. Nucl. Mater. 15 (1965) 298.
[9] D.F. Caroll, J. Am. Ceram. Soc. 46 (1963) 195.
[10] E.E. Jackson, M.H. Rand, Atomic Energy Research Establishment, Report AERE-R-3636, 1963.
[11] Z. Jin, Y. Du, Calphad 16 (1992) 355.
[12] H. Zhang, M.E. Huntelaar, R.J.M. Konings, E.H.P. Cordfunke, J. Nucl. Mater. 249 (1997) 223.
[13] M.E. Huntelaar, to be published.
[14] H. Zhang, M.E. Huntelaar, R.J.M. Konings, E.H.P. Cordfunke, J. Nucl. Mater. 250 (1997) 83.
[15] B. Schulz, G. Haase, in: Proceedings of the Ninth German–Yugoslav Meeting on Materials Science and Development, Hirsau, Stuttgart, 1989, 16–19 April.
[16] S. Burghartz, B. Schulz, J. Nucl. Mater. 212–215 (1994) 1065.
[17] K.A. McCarthy, S.S. Ballard, J. Opt. Soc. Am. 41 (1951) 1062.
[18] W.D. Kingery, J. Francl, R.L. Coble, T. Vasilos, J. Am. Ceram. Soc. 237 (1954) 107.
[19] J.L. Weeks, R.L. Seifert, Rev. Sci. Instrum. 24 (1953) 1054.
[20] F.H. Norton, W.D. Kingery, USAEC Report NYO-600, 1951, pp. 1–20.
[21] R.L. Rudkin, US Air Force Report ASD-TDR-62-24, Part II, 1963, pp. 1–16.
[22] R. Taylor, Appl. Phys. 16 (1965) 509.
[23] G. Jaeger, W. Koehler, F. Stapelfeldt, Ber. deut. Keram. Ges. 27 (1950) 202.
[24] K. Bakker, R.J.M. Konings, J. Alloys Comp. 271–273 (1998) 632.